06 Jul 2005

Multiphase Flow Packed-Bed Reactor Modeling: Combining CFD and Cell Network Model

Yi Jiang

Jing Guo

Muthanna H. Al-Dahhan
Missouri University of Science and Technology, aldahhanm@mst.edu

Recommended Citation

Y. Jiang et al., "Multiphase Flow Packed-Bed Reactor Modeling: Combining CFD and Cell Network Model," *Industrial and Engineering Chemistry Research*, vol. 44, no. 14, pp. 4940 - 4948, American Chemical Society, Jul 2005.
The definitive version is available at https://doi.org/10.1021/ie0491746

Multiphase Flow Packed-Bed Reactor Modeling: Combining CFD and Cell Network Model

Yi Jiang,*,† Jing Guo,‡ and Muthanna H. Al-Dahhan‡

Corning Inc., Science Center Drive, SP-TD-01-1, Corning, New York 14831, and Chemical Reaction Engineering Laboratory (CREL), and Department of Chemical Engineering, Washington University, St. Louis, Missouri 63130

The performance of a multiphase flow packed-bed reactor was evaluated by a mixing-cell network model in which the cell-scale flow field information was provided by multifluid CFD modeling. Such a sequentially combined modeling approach was able to show the heterogeneity of liquid species conversion in a trickle-bed reactor that has been confirmed by in situ magnetic resonance experiments.[1] A conventional plug flow model (PFM) and axial dispersion model (ADM) showed either overpredicted or underpredicted conversion compared with the conversion computed from the CFD-Cell Network model. Preliminary case study has shown the ability of the CFD-Cell Network model in assessing the impact of flow distribution on the trickle-bed reactor performance, which is a great help to trickle-bed reactor design and diagnosis.

1. Introduction

Multiphase flow packed-bed reactors have been employed extensively in the petroleum, petrochemical, chemical, bioprocessing, and waste treatment industries. The reactor-scale axial dispersion models (ADM)[2] and the particle-scale reaction−diffusion models[3−5] have been widely applied in trickle-bed reactor modeling by assuming simple flow patterns without solving detailed flow field. To account for the nonuniform flow patterns in reactor modeling, efforts have been made in the past couple of years for the two-region cell model,[6] cross-flow model,[7] the model based on liquid flow maldistribution,[8] the model with stagnant liquid zones included,[9] and the model with one-dimensional variations of gas and liquid velocities along the reactor.[10] The above ways of coupling multiphase flow pattern with chemical reaction(s), however, have not always led these models to being effective diagnostic tools for industrial trickle beds due to the complicated flow maldistribution impact on the reactor performance.

In principle, the performance of multiphase reactors can be predicted by solving the conservation equations for species mass, flow momentum, and thermal-reaction energy in combination with the constitution equations for species transport, chemical reaction, and phase transition. However, because of the incomplete understanding of the detailed physics, plus the nature of the equations, highly coupled and nonlinear, it is difficult to obtain the complete solutions unless one has reliable physical models, advanced numerical algorithms, and sufficient computational power. Although the full probability density function (PDF) method has some promises in solving the single-phase reactive flow,[11] for most multiphase reactive flow, the challenge exists in both numerical technique and physics understandings. The use of direct numerical simulation (DNS) in single particle and single void scale microflow modeling requires complete characterization of solids boundaries and voids configuration, which is obviously not practical for a reactor packed with massive particles. To focus on the macroscale flow distribution, a statistic method in implementing the porosity distribution has recently shown its promise in multiphase flow packed-bed modeling using ensemble-averaged equations of motion (i.e., multifluid computational fluid dynamics, CFD model).[12,13] The heterogeneity of porosity structure leads to the heterogeneity of gas and liquid flows. Thus, the next attempt is to utilize the obtained CFD flow distribution results to assess the impact of flow patterns on the reactor performance for given reaction kinetics. It was believed that nonuniform porosity distribution could lead to a nonuniform distribution of reactant phases and result in a nonuniform reactant conversion distribution in each cross section of the reactor. As a matter of fact, Yuen et al.[1] experimentally visualized the spatial variation of catalytic reaction conversion within a packed-bed reactor using in situ magnetic resonance (MR) for liquid-phase reaction of methanol and acetic acid. They found while the mean conversion increases along the direction of superficial flow, significant heterogeneity in conversion within each transverse section exists throughout the length of the bed due to the porosity heterogeneity.

In the Euler−Euler multifluid CFD model, the finite volume method is used to discretize the conservation equations of mass and momentum. The solutions of the continuous field phenomena (e.g., velocities, phase holdup, etc.) are represented by a discrete data set at certain spatial resolution. In other words, one may treat a packed bed as a network of interconnected discrete cells as illustrated in Figure 1. In a two-dimensional view, each cell has four vertexes and four faces. Each interior face is shared by two connected cells, and each interior vertex is common to four cells. After performing multifluid CFD flow simulation, one can obtain the phase volume fractions and the fluid interstitial velocities at each interior vertex of cells. Based on the mass balance of the fluid at each cell, the CFD flow field data

* To whom correspondence should be addressed. Tel: 607-974-9532. Fax: 607-974-3405. E-mail: jiangy@corning.com. This author was at Washington University in St. Louis when this work was done.

† Corning Inc.

‡ Chemical Reaction Engineering Laboratory (CREL), and Department of Chemical Engineering, Washington University.

10.1021/ie0491746 CCC: $30.25
Published on Web 02/11/2005

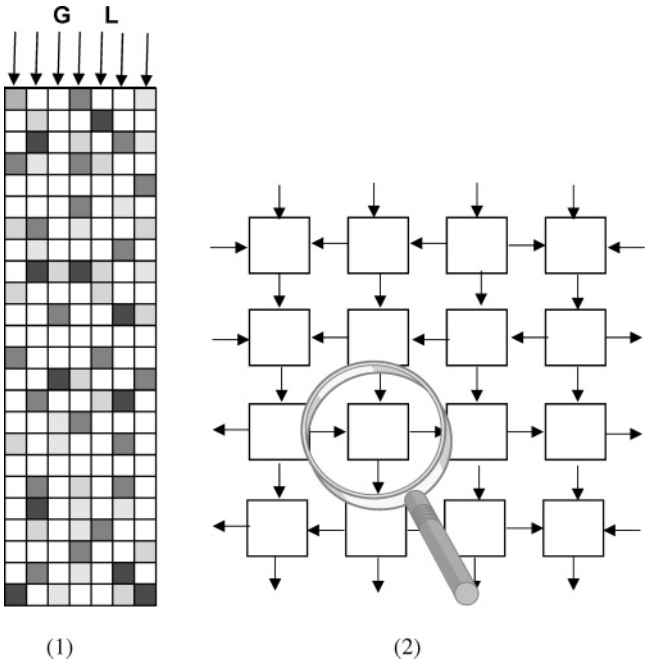

Figure 1. (1) Two-dimensional packed bed with gas and liquid cocurrent down flows and no-slip wall boundaries; (2) interconnected cell network.

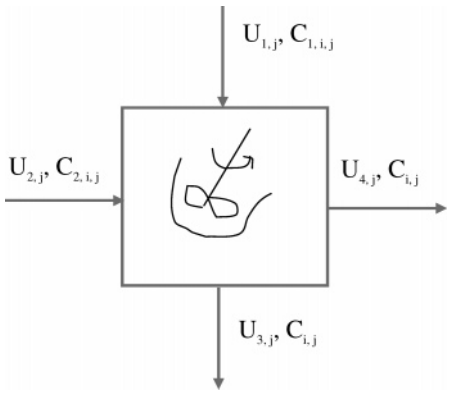

Figure 2. Fluid superficial velocities and concentrations of species i at the interior face of the cell j. The species concentrations in cell outflows are the same; therefore, the cell inlet species concentration has 3 subscripts while the cell outflow species concentrations only have 2 subscripts.

can be further converted into the phase volume fraction for each cell and into the fluid superficial velocity at each interior face of the cells as depicted in Figure 2.

One can track the concept of "cell network" of packed beds back to the early 1960s;[14] at that time the effluent of each cell was assumed to split into two streams, which were fed into the next row of cells. To allow the cell network be fed by the flow that modifies its value randomly as in a stationary Markov process, Krambeck et al.[15] suggested a general cell model, where a prior postulated network of channels connects the cells. In the two-dimensional array of cells, alternate rows are offset half a stage to allow for radial mixing. Jaffe[16] applied such a model in the heat release of a petroleum hydrogenation process and simulated the occurrence of steady state hot spots due to flow maldistribution. These discrete cell models involved the prediction of an infinite speed of signal propagation, which is not fundamentally correct as pointed out by Sundaresan et al.[17] Schnitzlein and Hofmann[18] then developed an alternative cell network model in which the elementary unit consists of an ideal mixer and a subsequent plug flow unit. The fluid streams are split or merged in infinitesimally small adiabatic mixing cells (without reaction), located between the different layers of elementary units. The fluid streams are split according to a constant flux through all elementary units, and the additional model parameter (δ) as a measure of the relative size of the two minireactors is needed. A prediction of the axial temperature profile for partial oxidation of methanol to formaldehyde by this cell model was found to be better than that by the continuum dispersion model. Later on, Kufner and Hofmann[19] incorporated the radial porosity distribution into the above cell model, which led to an even better agreement of the predicted temperature profile with the experimental data.

One should note that all these mentioned cell models were examined only for single-phase flow. Although they were claimed to be applicable for multiphase flow in principle, the heavy algebra largely diminishes the advantages of those models, particularly, when the complex bed structure and the complicated multiphase interactions need to be considered as that in the multifluid CFD modeling.

In this work, we have adopted the "discrete cell network" concept to describe the structure of packed-bed reactor. The multiphase flow distributions are modeled based on the structure heterogeneity of packed beds (i.e., porosity distribution) and the realistic interactions of fluid−fluid and fluid−particles. For example, the spatial distribution of fluid velocities is not obtained by the empirical flow-splitting rule as in those earlier cell network models, but is obtained from the solution of the multifluid CFD flow simulations without including reaction(s). The detailed description and discussion of the multifluid CFD model for multiphase flow in packed beds such as structure implementation, closures for multiphase flow equations, mesh dependency, and boundary conditions are available elsewhere.[12,13] The scope of this work is to illustrate the scenario of combined modeling schemes of multiphase flow and reaction kinetics, and to explore the advantages of such a modeling concept in the diagnostic analysis of the operating multiphase flow packed-bed reactors (e.g., trickle-bed reactors). Obviously, this approach is only applicable when gas and liquid flow distributions are NOT significantly affected by chemical reactions, which is true for most trickle-bed applications.

2. Multifluid CFD Model for Flow Simulation

A multifluid CFD model has been recently developed for packed beds to obtain the spatial distributions of flow velocity and phase volume fraction at certain spatial resolution provided that the porosity distribution at the same scale is known. The simulations are conducted by solving the ensemble-averaged mass and momentum conservation equations with the proper closures. The solution algorithm used is a cell-centered finite-volume method, which is implemented in CFDLIB codes developed by Los Alamos National Laboratory.[20] The essential two parts in adopting the multifluid CFD model for multiphase flow modeling in packed beds are (a) implementing the porosity distribution and (b) computing the momentum exchange coefficients, X_{kl}, for closures. To consider the effect of particle wetting on liquid distribution, the capillary pressure and particle fractional wetting of the external surface have been taken into account in cell-scale hydrodynamics calculations as shown in previous work.[12]

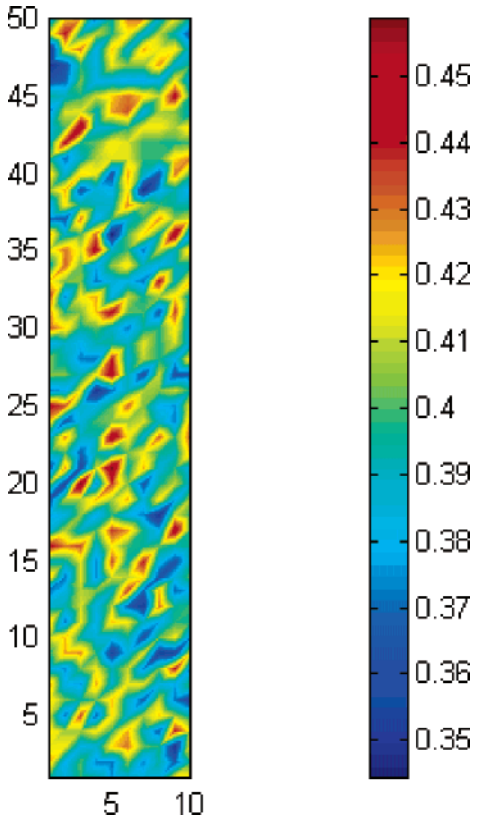

Figure 3. Porosity distribution at spatial resolution of 1 cm (d_p = 3 mm, L = 50 cm, D = 10 cm).

The existence of microscale turbulence in porous media has been detected by several experiments by point-wise probes;[21] therefore, one has to take the Reynolds stress term into consideration in the fine-mesh CFD modeling with high gas flow rate.[22] For the macroscopic flow modeling in packed beds, however, the contribution of the Reynolds stress term to fluid momentum equation is not important because when averaging a number of local (random) signals within a representative elementary volume (e.g., a cubic cell containing a cluster of particles), the microscopic turbulence is smoothed out.[12,23] Therefore, there has been no turbulence modeling included in this work.

The dependence of the flow solution on the grid size in multifluid CFD modeling had been checked in a previous paper. Apparently, the flow patterns did not significantly vary with changing the cell size from 1.0 to 0.5 cm; however, the more detailed flow characteristics were obtained in the fine-grid simulation. No significant variation in gas holdup predictions was found.[12]

Macroscopic flow velocity and phase volume fraction (holdup) distributions can be obtained by the multifluid CFD model provided that the following information on bed structure is available: (i) the mean porosity, (ii) the longitudinally averaged radial porosity profile if using a cylindrical column, and (iii) the distribution type and variance of cell porosity. Input information (i) and (ii) are available in the literature for most of the random packings.[24] Information (iii) is obtainable through Tomography techniques such as magnetic resonance imaging (MRI) measurement of the packed-bed structure.[25] The momentum exchange coefficients, X_{kl}, are computed by Ergun type of expressions developed by Holub et al.[26] and Attou et al.[27] for gas−liquid trickling flow regime.

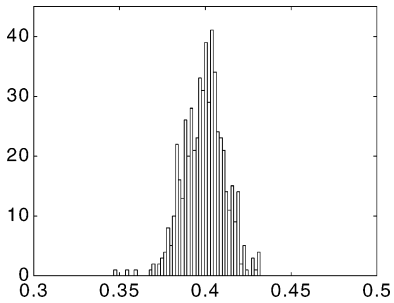

Figure 4. Histogram of porosity distribution (Gaussian distribution) used in multifluid CFD simulation (mean = 0.399; variance = 0.012).

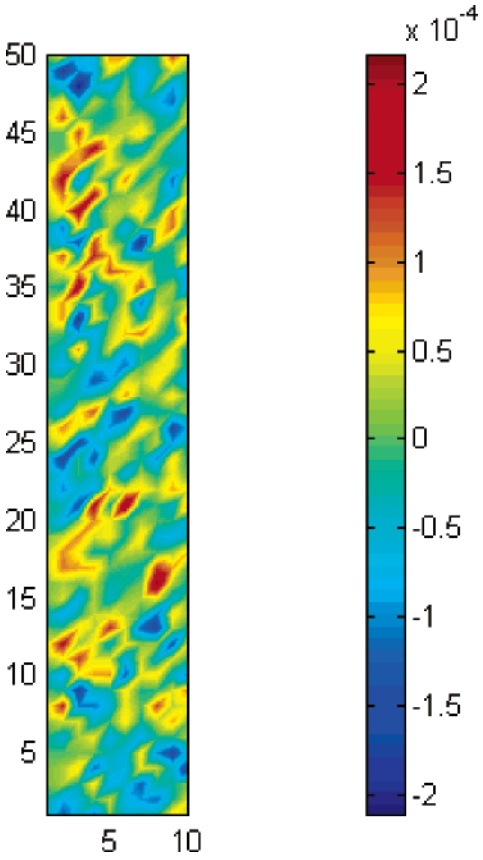

Figure 5. Simulated liquid superficial velocity component (U_x, m/s): U_{l0} = 0.003 m/s; U_{g0} = 0.06 m/s.

The detailed discussions of these issues are available elsewhere.[12]

A porosity contour generated based on a pseudo-Gaussian distribution is shown in Figure 3 in Cartesian coordinates.[28] This porosity distribution has a mean value of 0.399, a variance value of 0.012, and a longitudinally averaged horizontal profile of porosity which has a uniform value of 0.399 in this demo case [$\bar{\epsilon}(x) = 1/Lr\int_0^{Lr} \epsilon(x,y)dy$]. For a 2-D porosity distribution in $r-z$ cylindrical coordinates, the longitudinally averaged radial porosity profile has to follow those radial porosity profiles predicted by correlation.[12,24] The spatial resolution (i.e., discrete size) for this case is 1.0 cm, which is about three particle diameters (if d_p = 0.3 cm). The total number of discrete sections is 500 (10 in horizontal direction X, 50 in vertical direction Y). Figure 4 gives a histogram of 500 sectional porosity values. The multiphase flow simulation using a multifluid CFD model was based on such porosity distribution, which was input as the initial porosity value for each cell in solving

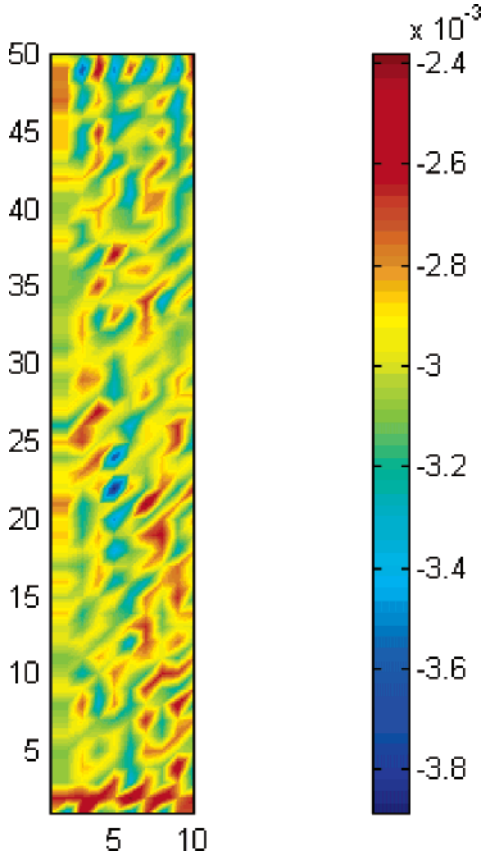

Figure 6. Simulated liquid superficial velocity component (U_z, m/s): $U_{l0} = 0.003$ m/s; $U_{g0} = 0.06$ m/s.

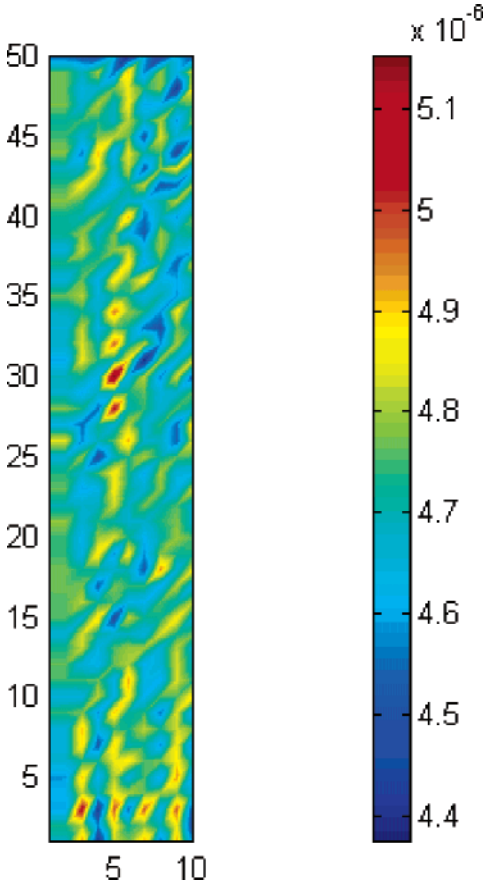

Figure 7. Computed cell-scale mass-transfer coefficient (k_{LS}, cm/s): $U_{l0} = 0.003$ m/s; $U_{g0} = 0.06$ m/s.

for ensemble-averaged three-phase mass and momentum equations. The momentum equation of the solid phase was turned off while solving the rest of the equations. Therefore, the porosity structure could be retained during the simulation.[12] Figures 5 and 6 exhibit the computed superficial liquid velocity components (U_x and U_z) at the same resolution as the porosity distribution. Since the mass-transfer coefficient of liquid to particle, k_{LS}, is a function of liquid superficial velocity, from the cell-scale liquid superficial velocity distribution given in Figures 5 and 6, one can compute the k_{LS} value at each cell based on the selected k_{LS} correlation,[29] and then come up with a contour plot of the k_{LS} value distribution as shown in Figure 7. It is obvious that the higher the cell liquid superficial velocity is, the higher the cell-scale liquid−solid mass-transfer coefficient is. We assume those mass-transfer correlations such as the k_{LS} correlation,[29] developed based on bench-scale packed-bed experiments, are valid at cell scale. In other words, the choice of cell scale has to be such that the cell still has representative features (gas, liquid, and solid phase). Typically, the cell scale should not be smaller than three particle diameters.

3. Mixing-Cell Network Model

To incorporate the mass-transfer impacts into the cell network model at the cell scale (i.e., a scale of a group particles; three times of particle diameters in this study), one needs to write the mass balance equations for the species in the gas and liquid bulk phase and at the catalyst surface. By assuming that each cell behaves in such scale like a well-mixed unit, the equations of species mass balances are essentially algebraic in nature, one can solve them sequentially from the inlet condition boundary.

For an irreversible solid catalyzed reaction between gaseous reactant A and liquid reactant B of the general form γA(g) + B(l) → P (l), the rate of reaction, per unit volume of the catalyst, is given by $\Omega = \rho_P k_r C_A^m C_B^n$.

The species concentration in gas and liquid streams leaving the jth cell through the kth face (*k-out*) is represented by $C^g_{A,j}$, $C^l_{A,j}$, and $C^l_{B,j}$ (they are "mixing-tank" concentrations, which are the same for all the streams leaving the cell j), and in the streams entering the jth cell through the kth face (*k-in*) is represented by $C^g_{A,k,j}$, $C^l_{A,k,j}$, and $C^l_{B,k,j}$. k is the face index with the stream entering the jth cell. The mass balances for species A and B for the jth cell then can be written as follows:

Species A, in bulk gas phase in jth cell

$$\sum_{k\text{-}in} U_{g,k,j} a_{k,j} C^g_{A,k,j} - C^g_{A,j} \sum_{k\text{-}out} U_{g,k,j} a_{k,j} = V_{c,j} (k_{GL} a_L)_{A,j} \left(\frac{C^g_{A,j}}{H_A} - C^l_{A,j} \right) \quad (1)$$

Species A, in bulk liquid phase in jth cell

$$\sum_{k\text{-}in} U_{l,k,j} a_{k,j} C^l_{A,k,j} - C^l_{A,j} \sum_{k\text{-}out} U_{l,k,j} a_{k,j} = V_{c,j} (k_{GL} a_L)_{A,j} \left(\frac{C^g_{A,j}}{H_A} - C^l_{A,j} \right) - V_{c,j} (k_{LS} a_S)_{A,j} (C^l_{A,j} - C^s_{A,j}) \quad (2)$$

Species A, at the catalyst particle surface in jth cell

$$(k_{LS}a_S)_{A,j}(C^l_{A,j} - C^s_{A,j}) = \gamma\rho_P k_{r,j}(1-\epsilon_j)(C^s_{A,j})^m(C^s_{B,j})^n\eta_{r,j}\eta_{CE,j} \quad (3)$$

Species B, in liquid phase in jth cell

$$\sum_{k\text{-}in} U_{l,k,j}a_{k,j}C^l_{B,k,j} - C^l_{B,j}\sum_{k\text{-}out} U_{l,k,j}a_{k,j} = V_{c,j}(k_{LS}a_S)_{B,j}(C^l_{B,j} - C^s_{B,j}) \quad (4)$$

Species B, at catalyst particle surface in jth cell

$$(k_{LS}a_S)_{B,j}(C^l_{B,j} - C^s_{B,j}) = \rho_P k_{r,j}(1-\epsilon_j)(C^s_{A,j})^m(C^s_{B,j})^n\eta_{r,j}\eta_{CE,j} \quad (5)$$

One can come up with following dimensionless quantities (6a−6p):

$$a_{g,j} = C^g_{A,j}/C^g_{A,0} \quad (6a)$$

$$a_{l,j} = H_{A,j}C^l_{A,j}/C^g_{A,0} \quad (6b)$$

$$a_{s,j} = H_{A,j}C^s_{A,j}/C^g_{A,0} \quad (6c)$$

$$b_{l,j} = C^l_{B,j}/C^l_{B,0} \quad (6d)$$

$$b_{s,j} = C^s_{B,j}/C^l_{B,0} \quad (6e)$$

$$u'_{g,k,j} = U_{g,k,j}/U_{g,0} \quad (6f)$$

$$u'_{l,k,j} = U_{l,k,j}/U_{l,0} \quad (6g)$$

$$\xi_{k-in,j} = a_{k-in,j}/a \quad (6h)$$

$$\xi_{k-out,j} = a_{k-out,j}/a \quad (6i)$$

$$\alpha_{A,j} = \frac{V_{c,j}(k_{GL}a_L)_{A,j}}{a_j U_{g,0}H_{A,j}} \quad (6j)$$

$$\alpha_{B,j} = \frac{V_{c,j}(k_{LS}a_S)_{B,j}}{a_j U_{l,0}} \quad (6k)$$

$$\beta_{A,j} = \frac{U_{g,0}H_{A,j}}{U_{l,0}} \quad (6m)$$

$$\gamma_{A,j} = \frac{(k_{LS}a_S)_{A,j}}{(k_{GL}a_L)_{A,j}} \quad (6n)$$

$$\gamma_{B,j} = \frac{(k_{LS}a_S)_{B,j}H^{m-1}_{A,j}C^g_{A,0}}{(k_{GL}a_L)_{A,j}C^l_{B,0}} \quad (6o)$$

$$k^*_j = \frac{\rho_P k_{r,j}(1-\epsilon_j)}{(k_{LS}a_S)_{A,j}}\left(\frac{C^g_{A,0}}{H_{A,j}}\right)^{m-1}(C^l_{B,0})^n \quad (6p)$$

By substituting the above dimensionless quantities (6a−6p) into species mass balance equations (1)−(5), one can get the following dimensionless equations (7)−(11).

$$\sum_{k\text{-}in} u'_{g,k,j}a_{g,k,j} - a_{g,j}\sum_{k\text{-}out} u'_{g,k,j} = \alpha_{A,j}(a_{g,j} - a_{l,j}) \quad (7)$$

$$\sum_{k\text{-}in} u'a_{l,k,j} - a_{l,j}\sum_{k\text{-}out} u'_{l,k,j} = \alpha_{A,j}\beta_{A,j}(a_{g,j} - a_{l,j}) - \alpha_{A,j}\beta_{A,j}\gamma_{A,j}(a_{l,j} - a_{s,j}) \quad (8)$$

$$(a_{l,j} - a_{s,j}) = \gamma k^*_j\gamma_A\eta_{r,j}\eta_{CE,j}a^m_{s,j}b^n_{s,j} \quad (9)$$

$$\sum_{k\text{-}in} u'_{l,k,j}b_{l,k,j} - b_{l,j}\sum_{k\text{-}out} u'_{l,k,j} = \alpha_{B,j}(b_{l,j} - b_{s,j}) \quad (10)$$

$$(b_{l,j} - b_{s,j}) = k^*_j\gamma_B\eta_r\eta_{CE,j}a^m_{s,j}b^n_{s,j} \quad (11)$$

Since we know from CFD flow modeling the inflow and outflow velocities of cell j ($u'_{g,k-in,j}$, $u'_{l,k-in,j}$, $u'_{g,k-out,j}$, $u'_{l,k-out,j}$). We also know the inflow species concentration ($a_{g,k-in,j}$, $a_{l,k-in,j}$, $b_{l,k-in,j}$) of cell j through the sequential cells' solution starting from the inlet boundary condition (i.e., marching the solution from the inlet layer of cells downward to the outlet layer), the variables to be solved are outflow species concentrations and species concentrations at the catalyst particle surface of cell j ($a_{g,j}$,$a_{l,j}$,$b_{l,j}$,$a_{s,j}$,$b_{s,j}$). For each cell, for example, for the jth cell, there are five equations with five unknowns. Note that the mass-transfer coefficient values ($\alpha_{A,j}$,$\alpha_{B,j}$,$\alpha_{A,j}\beta_{A,j}$,$\alpha_{A,j}\beta_{A,j}\gamma_{A,j}$) and the particle wetting degree ($\eta_{CE,j}$) are computed using bench-scale empirical correlations[2] based on cell-scale flow velocities and properties.

The computation scheme of the mixing-cell network model is straightforward. To obtain the species concentration for every cell interface in the 2-D reactor domain as shown in Figure 1, one needs to solve eqs 7−11 for all the cells. Basically, it can be done layer by layer starting from the top layer of the bed (inlet boundary condition) decided by inlet flow distributor(s). For a layer of cells there are normally four possible configurations of the inflow and outflow as shown in Figure 8 since for a packed bed with random packing we did not find major axial back-mixing; hence, it allows us to assume that "1" is always an inlet fact in cell j. A set of boundary conditions for flow velocities and species concentration are given at the first layer of cells (input cells, input conditions) as well as the cell conjunct to

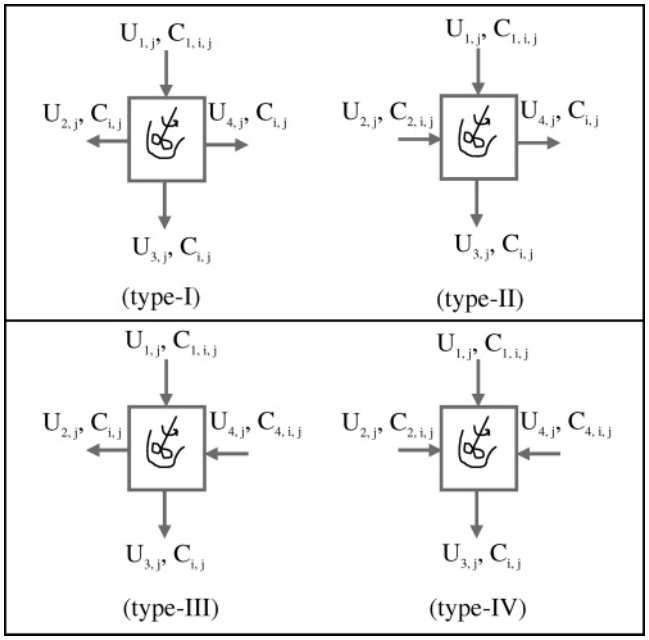

Figure 8. Two-dimensional cells with four possible inflow−outflow configurations (Cell-I: 3 outflows; cell-II and cell-III: 2 outflows; cell-IV: 1 outflow). The species concentrations in cell outflows are the same; therefore, the cell inlet species concentration has 3 subscripts while the cell outflow species concentrations only have 2 subscripts.

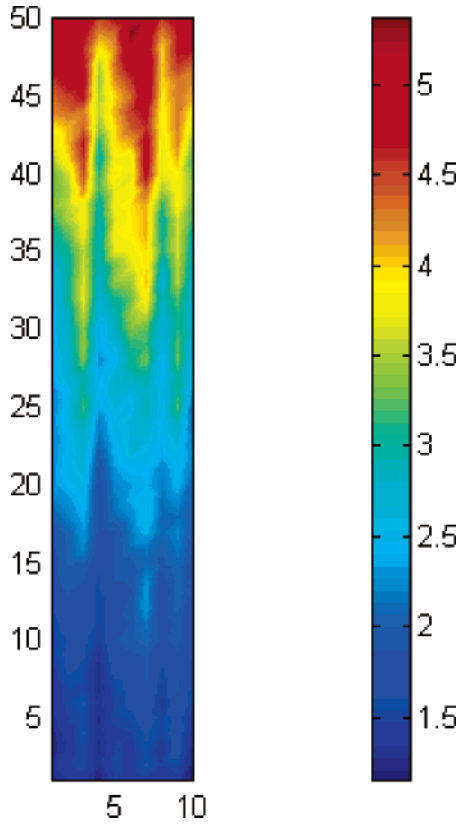

Figure 9. Concentration contour of species B in the liquid phase ($m = 0.0$; $n = 1.0$; $\gamma = 1.0$). $C^l_{B,0} = 5.0$ kmol/m^3; $U_{l0} = 0.003$ m/s; $U_{g0} = 0.06$ m/s.

Table 1. Case Study Conditions

reaction kinetics $\Omega = \rho_P k_r C_A^m C_B^n$	$m = 0.0$; $n = 1.0$; $\gamma = 1.0$; $\rho_p = 2500$ kg/m^3 $k_r = 1.0 \times 10^{-4}$ [m^3/kg·s][m^3/kmol]$^{m+n+1}$
inlet liquid concentration of species B	$C^l_{B,0} = 5.0$ kmol/m^3
inlet liquid superficial velocity	$U_{l0} = 0.003$ m/s
inlet gas superficial velocity	$U_{g0} = 0.06$ m/s
liquid-phase density	$\rho_L = 1000.0$ kg/m^3
gas-phase density	$\rho_G = 1.0$ kg/m^3
liquid-phase viscosity	$\mu_L = 1.0 \times 10^{-3}$ Pa·s
gas-phase viscosity	$\mu_G = 1.8 \times 10^{-5}$ Pa·s
Henry constant of species A	$H_A = 10.0$
molecular diffusivity of species A	$D_A = 7.86 \times 10^{-11}$ m^2/s
particle diameter	$d_p = 0.003$ m (sphere shape)
porosity of packed bed	mean: 0.399; variance: 0.012
mixing-cell size	cell area: $a = 1$ cm^2; cell volume: $V_c = 1$ cm^3

the walls. By solving such a set of algebraic equations layer by layer downward, one can get a whole set of solutions for species concentrations at the cell interface of the packed bed.

4. Case Study

The physical properties of the fluids and the relevant kinetics parameters are given in Table 1. For the purpose of concept demonstration, the reaction mentioned earlier has been used with the porosity structure presented in Figures 3 and 4. The CFD results presented in Figures 5 and 6 and the mass-transfer coefficients presented in Figure 7 are used in this case study. Figure 9 shows the calculated concentration distribution of species B in the liquid bulk phase while species A is in excess. Clearly, the modeling result shows

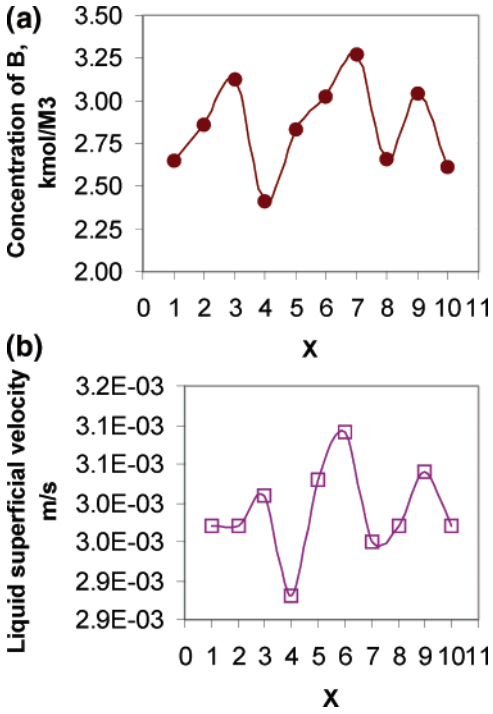

Figure 10. (a) Longitudinally averaged horizontal concentration profile of species B profile; (b) longitudinally averaged horizontal liquid superficial velocity profile. (C^l_B, filled circle; U_z, blank square; $C^l_{B,0} = 5.0$ kmol/m^3; $U_{l0} = 0.003$ m/s; $U_{g0} = 0.06$ m/s).

the concentration heterogeneity of liquid species B existing in a trickle-bed reactor even with uniform inlet flow distribution. Comparing Figure 3 (i.e., porosity contour) with Figure 9 (species B concentration contour), it is found that those relatively high concentration streams of species B occur in those zones with relatively high porosity. The pattern feature of liquid species B concentration looks similar to what Yuen at al[1] (see Figure 8 in article[1]) got from their MR visualization experiments for liquid trickling flow reaction system. Basically, the conversion of species B increases from the reactor top downward to the bottom. At each axial position (Y), there is significant heterogeneity in the conversion of species B, particularly in the first top-half of the reactor. Such conversion heterogeneity decreases at the bottom-half of the reactor.

Such species concentration contour provides great value for a diagnostic analysis of packed-bed reactor, in particular, when the bed structure and two-phase flow heterogeneities are encountered due to the changes in process operating conditions. Figure 10 shows the longitudinally averaged liquid flow velocity and the corresponded longitudinally averaged concentration profile of species B along horizontal (X) direction. As expected, the high liquid local superficial velocity leads to a lower liquid flow residence time and yields a lower conversion of species B.

We compared the computed concentration profiles of species B along the reactor from four different reactor models: (i) plug flow model (PFD), (ii) axial dispersion model (ADM) using axial dispersion coefficient calculated from the correlation given by Sater and Levenspiel,[30] (iii) mixing-cell network model based on CFD flow result, and (iv) axial dispersion model (ADM) using adjusted axial dispersion coefficient. As shown in Figure 11, it is obvious that the plug flow model gave an overpredicted conversion and the axial dispersion model gave an underpredicted conversion compared with CFD-

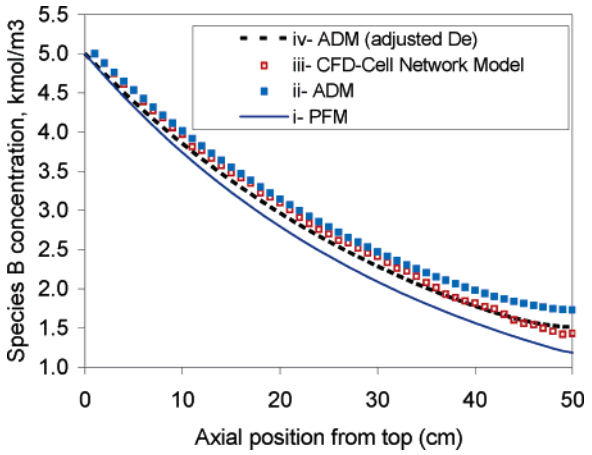

Figure 11. Calculated concentration profiles of species B at $k_r = 1.0 \times 10^{-4}$ m^3/kg·s, $n = 1.0$, $m = 0.0$ by (i) line: PFM; (ii) filled square: ADM ($D_e = 2.53 \times 10^{-4}$ m^2/s calculated from Sater and Levenspiel correlation,[30] $P_e = 5.92$); (iii) empty square: CFD-Cell Network model; (iv) dashed line: ADM (adjusted $D_e = 1.5 \times 10^{-4}$ m^2/s, $P_e = 10$). $C^l_{B,0} = 5.4$ kmol/m^3; $U_{l0} = 0.003$ m/s; $U_{g0} = 0.06$ m/s.

Cell Network model results. Even by adjusting the value of axial dispersion coefficient in model (iv), we could not get the model (iv) result to completely match the Cell Network model results. Single axial dispersion coefficient in the ADM model seems inadequate to characterize the effect of flow maldistribution on the reactor performance. On the other hand, the CFD-Cell Network model can not only provide the overall performance prediction but also provide a "numerical" way of visualizing the distribution of flow and species concentrations inside trickle-bed reactors, which is essential for reactor trouble-shooting and operational diagnosis.

5. Concluding Remarks

A new modeling concept of sequentially combining CFD flow field results and reaction kinetics computation through Cell Network has been developed for multiphase packed-bed reactors provided that the flow distribution is not significantly affected by chemical reaction(s) such as those in trickle beds. Such a combined modeling approach was able to show the heterogeneity of liquid species conversion in a trickle-bed reactor that has been experimentally confirmed by in situ magnetic resonance experiments.[1] The conventional plug flow model (PFM) and axial dispersion model (ADM) showed either overpredicted or underpredicted conversion compared with the conversion computed from the CFD-Cell Network model. Even tuning the axial dispersion coefficient, one-dimensional ADM still could not match the horizontal-averaged axial species concentration profile computed from the CFD-Cell Network model result. The preliminary case study has shown some promises that the CFD-Cell Network model can deliver the information on species concentration distribution together with multiphase flow distribution, which are critical to reactor design and reactor operational diagnosis. The CFD-Cell Network modeling for a system of complex kinetics are making progress with the concerns of species concentration distribution and of species selectivity distribution.

Although the CFD-Cell Network model showed qualitative agreement on the heterogeneity in conversion with MRI observation,[1] a quantitative comparison of this type of model with detailed experimental data is essential at some point in the future. Such model validation can be performed by implementing the measured bed porosity distribution of certain scale in CFD flow modeling to get the flow field results, and then incorporating known reaction kinetics into the Cell Network model with this flow field information, and computing the cell-scale species concentrations. Once we have experimental data of species concentration distribution, we can compare them with the modeling results. Basically in situ MRI seems a valuable means for such model validation.

Regarding the model application in the real world, the number of cells required for modeling an industrial-scale trickle-bed reactor, obviously, becomes very large if the same cell size (i.e., 1 cm in this case study) is used in CFD flow and Cell Network reaction modeling. By increasing the cell size, of course, one can use the model for a large-scale trickle-bed reactor but the resolution of the results may not be high enough, and one may loose certain insights into the modeling. For example, one may only capture the effect of the distributor on the flow and reaction distribution, but one may not be able to reveal the impact of those local porosities on the flow and reaction because the porosity distribution of cell scale will be uniform when the cell size is big enough. To be able to capture both large-scale flow pattern impact and local-scale porosity impact on reactor performance using the CFD-Cell Network model, a multilevel modeling scheme is necessary based on the balance of the information needed and the computation required. For example, one can group 10 cells by 10 cells into a zone of 100 cells. If the cell size is ~1 cm, then the zone size will be ~10 cm (you may not see any porosity maldistribution at this scale). One can run a "zone"-scale CFD flow modeling and get the flow information at ~10 cm scale and then use the Cell Network model to figure out the reactor performance at "zone" scale (~10 cm scale). For a typical zone, one can further run the cell-scale flow and reaction modeling within that zone (that is a total of 100 cells) to figure out detailed flow and reaction information within that zone. By looking at the "zone"-scale modeling results and the cell-scale modeling results in those typical zones, one can have the reactor information at two different levels.

While striving for solving multiphase reaction and multiphase CFD flow simultaneously in the reactors such as packed beds with very complicated flow domain, the developed CFD-Cell Network model perhaps provides a practical engineering approach in particularly for the system of complex reaction kinetics where the flow field is not significantly affected by reaction(s) going on in the reactors. In fact, there are many chemical reaction systems falling into this category. Even for the system with nonisothermal feature, one can develop an interactive CFD-Cell Network modeling scheme to get converged distribution solution of flow, species concentration, and temperature, which is a great help to identify the potential hotspots in trickle-bed reactors.

Although our case study has been focused on the trickle-bed reactors, as a general modeling concept, it can be extended to packed-bed reactors with other flow configurations such as gas−liquid cocurrent upflows and gas−liquid counterflows.

Acknowledgment

Special thanks go to Professor Milorad P. Dudukovic for constructive comments and valuable discussions. We

gratefully acknowledge the CREL industrial sponsors for financial support and Los Alamos National Laboratory for providing the CFDLIB code.

Nomenclature

a = a basis for cell cross-section area, m^2
$a_{k,j}$ = k interface area of cell j, m^2
$a_{g,j}$ = dimensionless concentration of A in the gas phase in cell j
$a_{l,j}$ = dimensionless concentration of A in the liquid phase in cell j
$a_{L,j}$ = gas−liquid mass-transfer area per unit cell volume in cell j, m^2/m^3
$a_{s,j}$ = dimensionless concentration of A at the particle surface in cell j
$C^g_{A,0}$ = concentration of A in the feed gas, $kmol/m^3$
$C^g_{A,k,j}$ = concentration of A in the gas phase entering the jth cell through the k face, $kmol/m^3$
$C^g_{A,j}$ = concentration of A in the gas phase leaving the jth cell, $kmol/m^3$
$C^l_{A,k,j}$ = concentration of A in the liquid phase entering the jth cell through the k face, $kmol/m^3$
$C^l_{A,j}$ = concentration of A in the liquid phase leaving the jth cell, $kmol/m^3$
$C^s_{A,j}$ = concentration of A at the particle surface, $kmol/m^3$, in cell j
$b_{l,j}$ = dimensionless concentration of B in the liquid phase in cell j
$b_{s,j}$ = dimensionless concentration of B at the particle surface in cell j
$C^l_{B,0}$ = concentration of B in the feed gas, $kmol/m^3$
$C^l_{B,k,j}$ = concentration of B in the liquid phase entering the jth cell through face k, $kmol/m^3$
$C^l_{B,j}$ = concentration of B in the liquid phase leaving the jth cell through k face, $kmol/m^3$
$C^s_{B,j}$ = concentration of B at the particle surface in the jth cell, $kmol/m^3$
D_e = effective intraparticle diffusivity of the species, m^2/s
H_A = Henry's law solubility coefficient of A, A_g/A_l
k_r = reaction-rate constant $[m^3/kg\cdot s][m^3/kmol]^{m+n-1}$
k^* = dimensionless rate constant
k_{GL} = gas−liquid mass-transfer coefficient, m/s (correlation given by Fukushima and Kusaka[31])
k_{LS} = liquid-solid mass-transfer coefficient, m/s (correlation given by Tan and Smith[29])
S_p = external surface area of a catalyst particle, m^2
U_g = superficial gas velocity, m/s
U_l = superficial liquid velocity, m/s
V_c = volume of cell, m^3
V_p = volume of a catalyst particle, m^3

Greeks

α_A, α_B = dimensionless gas−liquid mass-transfer coefficients defined by eqs 6j and 6k
β_A = parameter defined as in eq 6m
ϵ = void fraction in the jth cell
η_r = catalyst effectiveness factor, defined as $\eta_r = (1/\phi)\text{-}[(1/(\tanh 3\phi)) - (1/3\phi)]$
η_{CE} = catalyst particle wetting efficiency (correlation given by El-Hisnawi et al.[2])
γ = stoichiometric coefficient of A in the reaction
γ_A, γ_B = parameters defined as in eqs 6n and 6o
ρ = density of the catalyst particle, kg/m^3
ϕ = Thiele modulus for spherical catalyst particle
Ω = reaction rate per unit volume of catalyst particle, $kmol/m^3\cdot s$

Literature Cited

(1) Yuen, E. H. L.; Sederman, A. J.; Gladden, L. F. In situ magnetic resonance visualization of the spatial variation of catalytic conversion within a fixed-bed reactor. *Appl. Catal., A* **2002**, *232*, 29.

(2) El-Hisnawi, A. A.; Dudukovic, M. P.; Mills, P. L. Trickle-bed reactors: dynamic tracer tests, reaction studies, and modeling of reactor performance. *ACS Symp. Ser*. **1982**, *196*, 421.

(3) Beaudry, E. G.; Dudukovic, M. P.; Mills, P. L. Trickle bed reactors: liquid diffusional effects in a gas limited reaction. *AIChE J.* **1987**, *33*, 1435.

(4) Harold, M. P.; Watson, P. C. Bimolecular exothermic reaction with vaporization in the half-wetted slab catalyst. *Chem. Eng. Sci.* **1993**, *48*, 981.

(5) Guo, J.; Al-Dahhan M. A sequential approach to modeling catalytic reactions in packed bed reactors. *Chem. Eng. Sci.* **2004**, *59*, 2023.

(6) Brad Sims, W.; Gaskey, S. W.; Luss, D. Effect of flow regime and liquid velocity on conversion in trickle-bed reactor. *Ind. Eng. Chem. Res*. **1994**, *33*, 2530.

(7) Tasmatsoulis, D.; Papayannakos, N. Simulation of non-ideal flow in a trickle bed reactors by a cross-flow model. *Chem. Eng. Sci.* **1995**, *50*, 3685.

(8) Funk, G. A.; Harold, M. P.; Ng, K. M. A novel model for reaction in trickle bed with flow maldistribution. *Ind. Eng. Chem. Res*. **1990**, *29*, 738.

(9) Rajashekharam, M. V.; Jaganathan, R.; Chaudhari, R. V. A trickle-bed reactor model for hydrogenation of 2,4-dinitrotoluene: Experimental verification, *Chem. Eng. Sci.* **1998**, *53*, 787.

(10) Khadilkar, M. R. Performance studies of trickle bed reactors, D.Sc. Dissertation, Washington University in St. Louis, MO, 1998.

(11) Fox, R. O. Computational methods for turbulent reacting flows in the chemical process industry. *Rev. Inst. Fr. Pet.* **1996**, *51*, 215.

(12) Jiang, Y.; Khadilkar, M. R.; Al-Dahhan, M. H.; Dudukovic, M. P. CFD of multiphase flow in packed-bed reactors: I. k-Fluid Modeling Issues, *AIChE J.* **2002**, *48*, 701.

(13) Jiang, Y.; Khadilkar, M. R.; Al-Dahhan, M. H.; Dudukovic, M. P. CFD of multiphase flow in packed-bed reactors: II. Results and applications. *AIChE J.* **2002**, *48*, 716.

(14) Dean, H. A.; Lapidus, L. A computational model for predicting and correlating the behavior of fixed-bed reactors: 1. Derivation of model for nonreactive systems. *AIChE J*. **1960**, *6*, 656.

(15) Krambeck, F. J.; Shinnar, R.; Katz, S. Stochastic mixing models for chemical reactors. *Ind. Eng. Chem. Fundam.* **1967**, *6*, 276.

(16) Jaffe, S. B. Hot spot simulation in commercial hydrogenation processes. *Ind. Eng. Chem. Res*. **1976**, *15*, 410.

(17) Sundaresan, S.; Amundson, N. R.; Aris, R. Observations on fixed-bed dispersion models: The role of the interstitial fluid. *AIChE J.* **1991**, *26*, 529.

(18) Schnitzlein, K.; Hofmann, H. An alternative model for catalytic fixed bed reactors. *Chem. Eng. Sci.* **1987**, *42*, 2569.

(19) Kufner, R.; Hofmann, H. Implementation of radial porosity and velocity distribution in a reactor model for heterogeneous catalytic gas-phase reactions (TORUS-Model). *Chem. Eng. Sci.* **1990**, *45*, 2141.

(20) Kashiwa, B. A.; Padial, N. T.; Rauenzahn, R. M.; VanderHeyden, W. B. ASME Symposium on Numerical Methods for Multiphase Flows, Lake Tahoe, NV, 1994.

(21) Latifi, M. A.; Midoux, N.; Storck, A. The use of microelectrodes in the study of the flow regimes in packed bed reactor with single phase liquid flow. *Chem. Eng. Sci*. **1989**, *44*, 2501.

(22) Logtenberg, S. A.; Dixon, A. G. Computational fluid dynamics studies of fixed-bed heat transfer. *Chem. Eng. Process* **1998**, *37*, 7.

(23) Jiang, Y.; Khadilkar, M. R.; Al-Dahhan, M. H.; Dudukovic, M. P. Single phase flow modeling in packed beds: discrete cell approach revisited. *Chem. Eng. Sci*. **2000**, *55*, 1829.

(24) Benenati, R. F.; Brosilow, C. B. Void fraction distribution in beds of spheres. *AIChE J*. **1962**, *8*, 359.

(25) Sederman A. J.; Johns, M. L.; Bramley, A. S.; Alexander, P.; Gladden, L. F. Magnetic Resonance Imaging of liquid flow and pore structure within packed beds. *Chem. Eng. Sci.* **1997**, *52*, 2239.

(26) Holub, R. A.; Dudukovic, M. P.; Ramachandran, P. A. A phenomenological model for pressure drop, liquid holdup, and flow regime transition in gas−liquid trickle flow. *Chem. Eng. Sci.* **1992**, *47*, 2343.

(27) Attou, A.; Boyer, C.; Ferschneider, G. Modeling of the hydrodynamics of the cocurrent gas−liquid trickle flow through a trickle-bed reactor. *Chem. Eng. Sci.* **1999**, *54*, 785.

(28) Jiang, Y. Flow distribution and its impact on performance of packed-bed reactors, D.Sc. Dissertation, Washington University in St. Louis, MO, 2000.

(29) Tan, C. S.; Smith, J. M. Catalyst particle effectiveness with unsymmetrical boundary conditions. *Chem. Eng. Sci.* **1980**, *35*, 1601.

(30) Sater, V. E.; Levenspiel, O. Two-phase flow in packed beds: Evaluation of axial dispersion and holdup by moment analysis. *Ind. Eng. Chem. Fundam.* **1966**, *5*, 86.

(31) Fukushima, S.; Kusaka, K. Liquid-phase volumetric mass-transfer coefficient and boundary of hydrodynamics flow region in packed column with cocurrent downward flow. *J. Chem. Eng. Jpn*. **1977**, *10*, 467.

Received for review September 1, 2004
Revised manuscript received November 12, 2004
Accepted November 15, 2004

IE0491746